4th URSI AT-RASC, Gran Canaria, 19 – 24 May 2024

Two-Way Satellite Time and Frequency Transfer using an opensource, openhardware Software-Defined Radio platform

J. Achkar(1), É. Meyer(2), B. Chupin(1), F. Meyer(2), O. Chiu(1), M. Lours(1), J.-M. Friedt(2)
(1) LNE-SYRTE, Observatoire de Paris - Université PSL, CNRS, Sorbonne Université, Paris, France, Joseph.Achkar@obspm.fr
(2) LNE-LTFB, FEMTO-ST/OSU Théta, CNRS, Université de Franche-Comté, Besançon, France, jmfriedt@femto-st.fr

Abstract

Initial results of a portable (multiplatform) opensource, openhardware implementation of a pseudo-random binary number spectrum-spreading framework using Software Defined Radio for Two-Way Satellite Time and Frequency Transfer are given with a description of the hardware and software implementations. Satellite attitude measurements including ranging and velocity, as well as two-way transfer results, are presented.

1 Introduction

Two-Way Satellite Time and Frequency Transfer (TWSTFT) [1] is a primary technique in the computation of the Coordinated Universal Time (UTC), allowing time and frequency comparisons within and between continents. In addition to the current mainstream SATRE modem [2] used for communicating between a geostationary satellite and ground stations, various Software Defined Radio (SDR) receivers have been proposed to assess performance of digital links using modern signal processing framework. Indeed, SDR allows for collecting raw data and post-processing signal by using multiple algorithms, but most significantly to analyze the signals shared by all speakers using Code Division Multiple Access (CDMA) spectrum spreading during a given session, as opposed to the limited number of channels of a hardware implementation such as SATRE. Nevertheless, all current SDR projects remain closed source with either proprietary hardware implementation [3] or dedicated hardware requirements for real time processing. In this work, we aim at providing a platform independent implementation of a free and opensource/openhardware SDR framework, including **emitter** and receiver, for assessing the various communication parameters of a TWSTFT link. After describing the various station implementation tested on a practical link, we demonstrate link budgets, time and frequency transfer link stabilities and resolutions.

2 Emitter and receiver architectures

Time transfer requires spectrum spreading since range resolution is classically known from the RADAR equation to be inverse of the bandwidth. From the implementation of GPS L1 C/A or SATRE modem implementation, it is known that Binary Phase Shift Keying (BPSK) modulation of the 70 MHz Intermediate Frequency (IF) carrier allows for achieving time transfer with a resolution given by the inverse of the chip rate. Furthermore, correlation peak fitting allows for improving the time resolution by a factor equal to the Signal to Noise Ratio (SNR), leading to subns resolution with 5 MHz sampling rate on a 4-MHz wide Radio-Frequency (RF) channel.

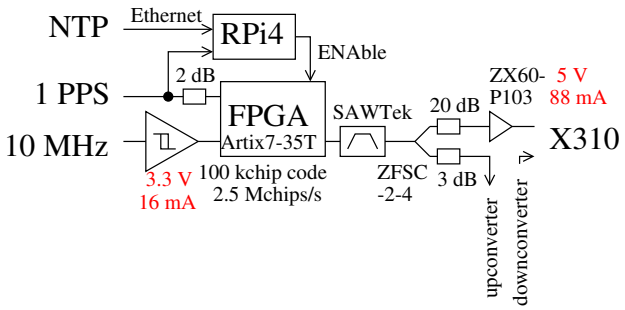

Figure 1. Outline of the hardware with a dual coherent receiver fetching the reference signal straight from the emitter and the measurement signal from the downlink after frequency conversion from 11 GHz to the 70 MHz IF (not shown).

Our implementation of this communication scheme aims at flexibility and reconfigurability as proposed by SDR: all signal generation is handled by a Field Programmable Gate Array (FPGA) with a minimum of hardware peripheral components added for meeting spectral occupation specifications – in our case only a Surface Acoustic Wave (SAW) bandpass filter centered on the 70 MHz IF and attenuators prior to feeding the upconverter of the Very Small Aperture Terminal (VSAT) classically fitted to the SATRE modem. The implementation has been demonstrated on the Zynq 7020 of the Zedboard, the Spartan6 of the Ettus Research B210 and the Kintex7 of the Ettus Research X310 with a single gateware description using the Python based language Amaranth (`https://github.com/amaranth-lang`), although all results shown in this presentation result from pseudo-random number (PRN) sequences generated on the Artix-7 of the Digilent Cmod-A7 board (Fig. 1).

Considering the tremendous increase in computational power, an investigation on the various code lengths has shown [4] no impact on the time transfer stability, the improved SNR brought by the increased pulse compression ratio associated with long codes being compensated for by the fewer averages with a given exchange sequence. We have selected a 100 kchip-long code at a rate of 2.5 Mchips/s in order to reduce the Pulse Repetition Interval (PRI) and hence the range uncertainty since delays on a baseline as wide as Western Europe exceed the 4 ms PRI of the 10 kchip-long SATRE code. We have selected 17-bit long maximum-length sequence Galois-field PRN sequences with arbitrary seeds 09 and 15 for generating orthogonal codes. Increasing the PRI does reduce the digital communication datarate though, with the SATRE communicating 250 bits/s HiRate data whereas our implementation is limited to 25 bits/s holding the NTP second encoded as 8-bit binary format, least significant bit first after a start bit.

3 Link budget and signal to noise ratio

Various link budget indicators are needed, with most commonly the received signal power and SNR. While the total received signal power is the variance of the $I + jQ$ datastream, this information is irrelevant in the case of CDMA communication when multiple emitters broadcast on the same carrier frequency. Hence, individual transmitted code identification is needed to assess the link budget with each transmitting station. The objective of the processing sequence is to extract the signal component of each code using the following algorithm (Fig. 2):

1. the time delay between the local copy of the code and the received signal is computed from the cross-correlation, possibly with some oversampling to identify the delay with sub-sampling period resolution
2. the local copy of the code is rotated by the resulting time delay and the received signal multiplied with this binary sequence, resulting in spectrum de-spreading by cancelling the BPSK modulation
3. the signal is the square of the mean value of the despread signal
4. the noise is the variance of the despread signal.

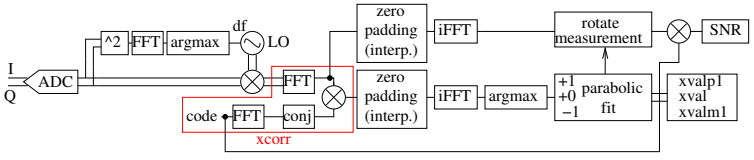

Figure 2. Outline of the signal processing algorithm on the receiver module.

We assess the SNR computation by comparing this quantity computed at the remote end of the link, on the receiver module, with the output power measurement as observed by a microwave sensor on the emitter module. Excellent agreement is observed between the two quantities (Fig. 3).

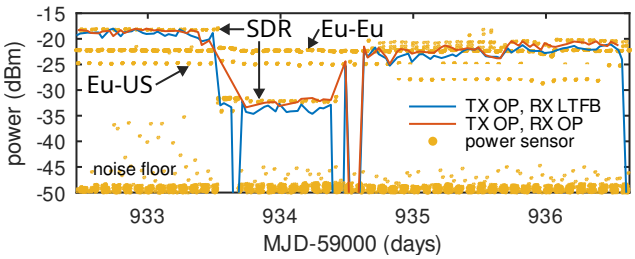

Figure 3. Comparison of the SDR power estimate (blue, red in two-way and ranging measurements) with respect to a reference microwave power sensor located at the input port of the transmitting parabola at LNE-SYRTE (OP).

In the context of SDR, the objective is to get rid of unstable analog components to rely solely on reproducible and deterministic digital signal processing. Nevertheless, due the discrete time emitted signal generation, unwanted spectral components are generated from the Digital to Analog Converter (DAC) which are filtered at the output of the General Purpose Input/Output (GPIO) pin of the FPGA before feeding the microwave upconverter and amplifier for broadcasting to the geostationary satellite. SAW filters have been selected to efficiently (> 50 dB) unwanted spectral components with insertion losses (≤ 25 dB) low enough to keep the generated signal above the targeted level of -20 dBm as typically generated by the SATRE modem to feed the VSAT emitter.

SAW filters being based on the conversion of electromagnetic waves to acoustic waves propagating on piezoelectric substrates prone to thermal drift, the impact of this analog components on the link delay must be assessed. Two filters were selected, C-Tech 321823 and SAWTEK 851547, both documented as 70 MHz IF bandpass filter with 2.5 MHz bandwidth. Both filters exhibit similar insertion losses (21.5 dB and 25.2 dB nominal losses respectively) but their temperature behavior and group delay are different. The former filter manufactured on lithium tantalate exhibits a nominal 4.9 μs group delay with a temperature sensitivity of 20 ppm/K while the former is documented to exhibit a 2.3 μs group delay and undocumented temperature sensitivity but its design on a quartz substrate would be compatible with a turnover temperature at room temperature and hence negligible first order temperature sensitivity. In all cases the time delay introduced by the SAW filter is expected to be in the picosecond range under the controlled environmental conditions of a TWSTFT setup, but with variations documented from filter to filter to be in the tens of nanoseconds.

4 Digital signal processing

The core concept of time transfer is cross correlation *xcorr*, and its practical implementation through the Fast Fourier

Transform FFT following the application of the convolution theorem stating that $FFT(xcorr(x,y)) = FFT(x) \cdot FFT^*(y)$ for matching the pseudo random sequence x locally generated and the remote signal y. Extending the code duration for improving the SNR requires expanding computational capability as the load of a Fast Fourier Transform on N samples rises as $N\log_2(N)$.

We have selected a post-processing approach running on generic processing hardware (e.g. not requiring dedicated GPU hardware) in order to identify all communicating stations with no restriction on the number of channels processed during each session.

Digital signal processing holds the promises of reproducible results since digital algorithm execution is independent on environmental conditions (analog processing) or implementation. Despite floating point number description being inaccurate, the various proposed implementations in GNU/Octave, Python using FFTW or Numpy, and C++ all match to better than the 10th decimal or the hundred of ps.

5 Time and Frequency Transfer results

A two-week long TWSTFT session was completed using the same hardware setup located at LNE-SYRTE (OP) and LTFB. In both setups, the Artix-7 FPGA is clocked by the reference input 1-PPS and 10 MHz, with a PLL generating the 280 MHz signal clocking the PRN generator and the 70 MHz carrier spread by the BPSK modulation. Two Basic RX daughter boards with only a balun and no active frequency shifting are fitted on Ettus Research X310 receivers. The two channels are used on the one hand to collect on the reference channel the 70 MHz signal driving the upconverter as a loopback reference signal, and on the other channel the 70 MHz signal received by the downconverter.

Ranging and two-way signals have been collected and each correlation peak is timestamped on each reception site. The two-way analysis requires that the difference computation on the remote signal to loopback time difference computed at each end is performed at the same time so that the satellite motion contribution is cancelled. Because we have selected post-processing, the data storage is plagued by uncontrolled latencies including digital communication over Ethernet and file storage under supervision of a general purpose multitasking operating system with measurement sequences triggered by a mechanism – crontab – with poor timing resolution. The PRN synchronization on both link ends has been solved by using a single board Raspberry Pi 4 computer to actively probe the 1-PPS reference input on the one hand, and NTP synchronized to better than 1-second its real time clock. By detecting the rising edge of the 1-PPS prior to the start of the next communication session, the FPGA emission is enabled but only starts on the next rising edge of the 1-PPS. Under the assumption that the 1-PPS reference signal between both stations is aligned to better than a few milliseconds, the satellite motion of a few ns/s induces a TWSTFT processing error in the picosecond range, negligible in the current application.

Figure 4 summarizes the result of a two-week TWSTFT measurement performed during the odd UTC hours between min 4 to min 9 and min 46 to min 51, each session lasting 5 minutes. From top to bottom:

1. the uncalibrated TWSTFT measurement ;
2. the standard deviation within each 5-minute long session of the remote communication after removal of the parabolic trend. The OP standard deviation is larger due to a weaker power feeding the loopback channel (-14 dBm), while the LTFB loopback gain was tuned to benefit from the full scale range of 6 dBm of the X310 analog to digital converter. In all cases the standard deviation within each 5-minute session remains below 1 ns ;
3. the satellite motion velocity as measured with the slope of the remote communication signal, emphasizing the need for synchronizing the two ends of the communication link to sub-100 ms to reach sub-nanosecond stability from one session to the next since the satellite motion can reach up to 4 ns/s ;
4. the frequency offset with respect to the nominal 70 MHz IF carrier, including the Doppler shift from the satellite motion and the satellite transponder frequency shift.

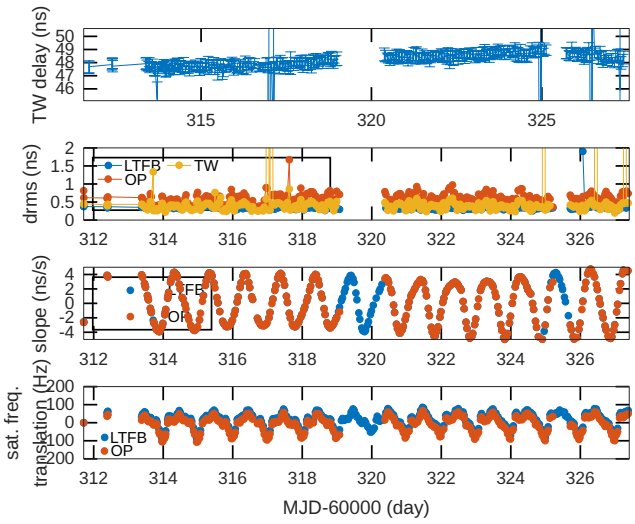

Figure 4. Two-week TWSTFT measurements between OP and LTFB using SDR emitter and receiver.

The SNR during these sessions is comparable with those classically exhibited by the SATRE modem, converted to a $C/N0$ value by adding the 67 dB of the 5 MHz channel bandwidth to reach values between 52 to 56 dB.Hz (Fig. 5).

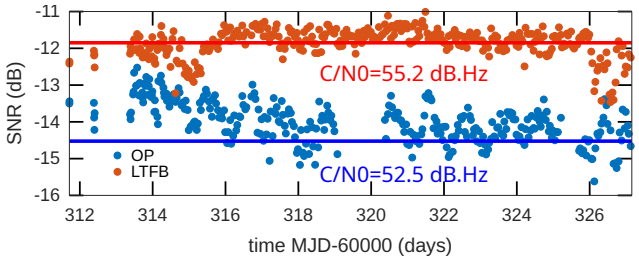

Figure 5. Signal to noise ratio at OP (blue) and at LTFB (red) during the same measurement session than displayed in Fig. 4.

6 Comparison between the SDR and SATRE TWSTFT

The Timetech SATRE modem is the TWSTFT reference instrument and the proposed solution is compared with the operational link between OP and LTFB. The SATRE communication is performed at the end of each UTC even hour while the SDR communication is performed at the beginning and end of each odd UTC hour. The SATRE communication lasts 3 minutes of which the last 2 minutes are used for TWSTFT analysis, while the whole 5 minute exchange of SDR is processed and used in the analysis.

The time-evolution of the comparison is exhibited in Fig. 6, with a close match of the observations by both instruments. The SDR link failed twice during the two-week sessions, in both cases with the X310 failing to transfer the expected number of samples to the recording GNU Radio script and the interface remaining busy during the subsequent link schedules.

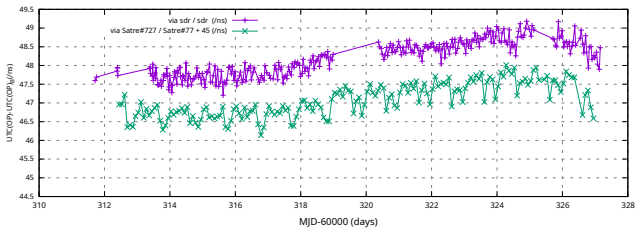

Figure 6. Time evolution of the SDR TWSTFT link (purple) and SATRE link (green), offset to match the arbitrary time delay of the uncalibrated SDR measurement.

Detailed statistical analysis are currently underway.

7 Conclusion

We have demonstrated a functional, portable implementation of SDR emitter and receiver pairs for TWSTFT. Results on par with commercial proprietary hardware have been demonstrated, with an openhardware architecture targeted towards further improvements by the relevant communities. First results on the OP-LTFB link were presented, showing measurement fluctuations well below 500 ps over several days and a signal to noise ratio in the 52 to 55 dB.Hz range.

As introduced, the proposed scheme is inspired by technology from the 1970s and 1980s with the use of the BPSK modulation for communicating through the satellite link. Global Navigation Satellite Systems (GNSS) have shifted to improved modulation schemes (BOC), improving spectral efficiency and improving digital communication performance using Forward Error Correction (FEC) whose investigation is perfectly suited to the opensource implementation of the TWSTFT platform. Further investigation will hence focus on improved modulation schemes and codes aimed at improving cross-code interference and timing resolution.

All software for reproducing the proposed setup is available at `https://github.com/oscimp/amaranth_twstft`

Acknowledgements

This work is supported by the French National Research Agency ANR through the OscillatorIMP (Oscimp) and FIRST-TF grants. C. Calosso (INRIM, Italy) provided the SNR calculation algorithm and motivated stimulating discussions. Nathan Gallone contributed the Amaranth software as part of his internship visit at FEMTO-ST. Maxime Dupont contributed on the OP side and Gwenhael Goavec-Merou on the LTFB side in establishing this link and developing the FPGA gateware.

References

[1] The operational use of two-way satellite time and frequency transfer employing pseudorandom noise codes. Recommendation ITU-R TF.1153-4. 08 2015.

[2] Ph Hartl. Present state of long distance time transfer via satellites with application of the mitrex-modem. In *MILCOM 1986-IEEE Military Communications Conference: Communications-Computers: Teamed for the 90's*, volume 2, pages 29–3. IEEE, 1986.

[3] Zhiheng Jiang, Victor Zhang, Yi-Jiun Huang, et al. Use of software-defined radio receivers in two-way satellite time and frequency transfers for UTC computation. *Metrologia*, 55(5):685, 2018.

[4] J-M Friedt, Michel Lours, Gwenhaël Goavec-Merou, et al. Development of an opensource, openhardware, software-defined radio platform for two-way satellite time and frequency transfer. In *Joint EFTF/IFCS*, pages 1–4. IEEE, 2023.